Design of a coil for electromagnetic levitation: comparison of numerical models and coil realization

Romain Pons, Annie Gagnoud, Didier Chaussende, Olga Budenkova

▶ **To cite this version:**

Romain Pons, Annie Gagnoud, Didier Chaussende, Olga Budenkova. Design of a coil for electromagnetic levitation: comparison of numerical models and coil realization. Magnetohydrodynamics c/c of Magnitnaia Gidrodinamika, 2022, 58 (1/2), pp.55-64. 10.22364/mhd . hal-03739247

HAL Id: hal-03739247
https://hal.science/hal-03739247v1

Submitted on 27 Jul 2022

HAL is a multi-disciplinary open access archive for the deposit and dissemination of scientific research documents, whether they are published or not. The documents may come from teaching and research institutions in France or abroad, or from public or private research centers.

L'archive ouverte pluridisciplinaire **HAL**, est destinée au dépôt et à la diffusion de documents scientifiques de niveau recherche, publiés ou non, émanant des établissements d'enseignement et de recherche français ou étrangers, des laboratoires publics ou privés.

DESIGN OF A COIL FOR ELECTROMAGNETIC LEVITATION: COMPARISON OF NUMERICAL MODELS AND COIL REALIZATION

R. Pons*, A. Gagnoud, D. Chaussende, and O. Budenkova

Univ. Grenoble Alpes, CNRS, Grenoble INP, SIMAP, F-38000 Grenoble, France
*Corresponding author's e-mail: romain.pons1@grenoble-inp.fr

Key words: numerical modeling, home-code, coil optimization, stable equilibrium position

Abstract

The idea of optimization of electromagnetic coil for levitation under terrestrial conditions using analytical approach or numerical simulations seems attractive, yet, formulation of such problem is not straightforward. As a first step toward it, analytical and numerical modeling for the real electromagnetic inductor are performed using 2D and 3D presentation of the latter with analysis for the equilibrium position of samples of various sizes, their temperature and the symmetry of the fluid flow. Results obtained numerically are compared with experimental observations.

Introduction

Electromagnetic levitation (EML), allows one to hold in space an electrically conductive sample both in its solid and liquid state, without having any contact with it and thus preventing its contamination. EML is widely applied in material science, both in microgravity and in terrestrial conditions [1-5]. Combination of EML with microgravity is advantageous since it permits reducing of electromagnetic forces and the liquid sample tends to keep spherical shape. Moreover, geometry of the electromagnetic (EM) inductor can be simplified and optimized to approach the axially symmetric electromagnetic field. However, experiments in microgravity are expensive and hard to get. Similar studies can be done under terrestrial conditions, yet, design of a coil for levitation becomes a delicate task. Indeed, the gravity has to be overcome and transition to liquid state should be assured for wide range of sample sizes and variety of material properties along with minimal deformation of the liquid droplet. Moreover, it is essential to get a good visibility of the levitating sample during the experiment. One can assume that analytical or numerical analysis can help in coil design, yet, formulation of the corresponding optimization problem is not straightforward. The present study served several aims. First, it allowed us to estimate at which extent the axially symmetric presentation of the inductor, both analytical and numerical, can help in analysis of a real inductor. Second, it is shown that the 3D simulations which account for the exact geometry of a real inductor could be achieved and that they provided information about 3D effects thus giving some ideas regarding optimization problem to obtain levitation with desired characteristics. Equilibrium position of a spherical sample and the temperature of the latter, determined via numerical modeling, are compared with the data obtained from experimental observation. Finally, a home-made code for electromagnetic calculations is validated.

Numerical modeling

The analytical approach for modeling of the electromagnetic inductor is detailed in [6] and is based on solutions obtained elsewhere [7]. It is assumed that the EM coil consists of

coaxial circular loops defined by their radius and axial position (b_i, z_i) with the effective AC current I_{eff} circulating in each loop with the frequency f. Then, the effective magnetic field created by the coil along the central axis of the coil, $H(z)$ can be defined as a superposition of the magnetic fields produced by each of the loops via eq.(1):

$$H(z) = \frac{1}{2} I_{eff} \sum_{n=1}^{N_{pos}} \frac{b_n^2}{(b_n^2 + (z - z_n)^2)^{3/2}} - \frac{1}{2} I_{eff} \sum_{n=1}^{N_{neg}} \frac{b_n^2}{(b_n^2 + (z - z_n)^2)^{3/2}} \qquad (1)$$

where N_{pos} and N_{neg} represent number of turns and counter-turns, i.e. the number of coils with opposite circulation direction of the electric current.

Let a spherical sample with the radius a, electrical conductivity σ_e and the magnetic permeability $\mu = \mu_0$ is placed at the coil's axis, here $\mu_0 = 4\pi \cdot 10^{-7}$ H.m^{-1} is the magnetic permeability of the vacuum. Then the resulting axial force $F_z(z)$ acting on the sample and depending on its axial position z, and the total Joule power $Q_J(z)$ dissipated in the sample are given by the eq.(2) and eq.(3) respectively:

$$F_z(z) = 2\pi\mu \, H(z) \, dH(z)/dz \; G_1 \qquad (2)$$

$$Q_J(z) = 2 \cdot \; 3\pi \, a \; H(z)^2/\sigma_e \; G_2 \qquad (3)$$

with

$$G_1 = 1 - 3\,[\sinh(2x) - \sin(2x)]/[4x(\sinh(x)\sinh(x) + \sin(x)\sin(x))]$$

$$G_2 = [x(\sinh(2x) + \sin(2x)) - \cosh(2x) + \cos(2x)]/(\cosh(2x) - \cos(2x))$$

where the functions $G_1 = G_1(x)$ and $G_2 = G_2(x)$ depend on the non-dimensional parameter defined as a ratio of the sample radius to the electromagnetic skin depth: $x = a(\pi\mu f\sigma_e)^{1/2}$. Note an additional factor 2 in eq.(3) compared to the eq.(14) from the ref. [6] because the function $H(z)$ calculated with the eq.(1) gives the *effective* value of the magnetic field.

The equilibrium vertical position of the sample inside the coil can be calculated from the balance of the forces acting on the sample, which are gravity and the Lorentz force. The average temperature of the sample can be obtained if the boundary conditions for the sample cooling are known. Here, a radiative heat exchange between the sample and the environment having the temperature T_{env} is taken into account.

Numerical modeling in 2D and 3D is performed with a home-made code MIMEF and with COMSOL Multiphysics® software. MIMEF is a code dedicated for modeling of large variety of inductive processes [8]. The advantage of the MIMEF code consists in coupling of the Integral Method (IM), used for calculation of EM fields, with Finite Element Method (FEM), which is used for calculation of heat transfer and fluid flow in the load. In particular, utilization of IM limits electromagnetic calculations only to the electrically conductive elements. The EM model is based on the Ohm's law and the conservation of the electric current, both laws are written with use of complex variables. The density of the electric current $\boldsymbol{j}$ is related to the vector potential via the Biot-Savart equation, details can be found elsewhere [8]. Once the solution for the EM problem is found, the distribution of the volume density of the Lorentz force f_L and of the Joule power q_{th} inside the sample are calculated in a standard way, and the total effective values of the Joule heating Q_{th} and axial component of the Lorentz force $F_{L,z}$ are obtained with the integration over the sample volume V_s :

$$q_{th} = \boldsymbol{j} \cdot \boldsymbol{j}^*/(2\sigma_e), \qquad Q_{th} = \iiint_{V_s} q_{th} dv \qquad (4)$$

$$\boldsymbol{f}_L = \mathrm{Re}(\boldsymbol{j} \times \boldsymbol{B}^*)/2, \qquad F_{L,z} = \iiint_{V_s} f_{L,z} dv \tag{5}$$

where the sign $*$ stands for the complex conjugate, $\boldsymbol{B}$ is the complex vector for magnetic induction found in numerical solution and Re corresponds to the real part of a complex number. To compare results with the analytical solution, 2D calculations with MIMEF are made for various axial position of the sample inside the coil. The modeling in COMSOL Multiphysics® is performed with the use of the modules "Magnetic Field", "Heat Transfer" and "CFD", which are coupled with use of the "Multiphysics" option. Electromagnetic calculations are done in frequency domain, then the Lorentz force and Joule power are used for calculations of the fluid flow (k-ε low Re) and temperature distribution inside the sample. In electromagnetic calculations the accessory named "coil" is used which is excited by applying an external current whose amplitude is taken equal to $\sqrt{2}I_{eff}$. Details of approach and model realization can be found in documentations of COMSOL Multiphysics® [9] and are omitted here for the sake of brevity. Similar to calculations with MIMEF, different axial position of the sample are considered in 2D calculations, and obtained volume density of the Lorentz force and Joule heating are integrated over the sample volume in order to compare them with the analytical approach. Modeling in 3D is performed with variation of the sample position over all spatial coordinates.

The equilibrium position of the sample can be found through the balance of the total electromagnetic force acting on the sample and the gravity force, [$\sum$ F = 0]. Otherwise, the equilibrium position of the sample can be defined as a location where the energy of the system W composed of the energy of the gravity W_g and the electromagnetic field W_{em} (eq.6) has the minimal value, the latter is sought with the simplex algorithm:

$$\mathrm{W} = \mathrm{W_g} + \mathrm{W_{em}} = Mgz - \iiint_{\Omega} \frac{1}{4\mu_0} \mathrm{Re}(\boldsymbol{B} \cdot \boldsymbol{B}^*) dv \tag{6}$$

here the integration is performed over the whole calculation domain Ω .

Physical and geometrical parameters

Simulations are performed for a coil made of copper whose electric conductivity is taken as $\sigma_{coil} = 5.997 \cdot 10^7 \Omega^{-1}.\mathrm{m}^{-1}$, with the effective current circulating in the coil $I_{eff} = 380$ A with frequency $f = 140$ kHz. As a charge, a sample of Ni is considered whose properties are given in the Table 1, we considered three sizes of the sample: $a = 2.5$ mm, 3 mm and 3.5 mm.

Table 1: Properties of the sample

Properties	Symbol	Unit	Value [10]
Density	ρ	$kg\ m^{-3}$	7905
Thermal conductivity	k_{th}	$W\ m^{-1}\ K^{-1}$	65.7
Electrical conductivity	σ_e	$\Omega^{-1}\ m^{-1}$	1.18×10^6
Emissivity	ε	-	0.33
Viscosity	μ	$Pa.s$	4.58×10^{-3}
Melting point	T_f	K	1728

A real 3D inductor (Table 2, fig. 1) presents helicity and has a current reversal loop that could not be reproduced in the axisymmetrical 2D model. Consequently, the coil in 2D is based on the 3D geometry of the latter as follows: the radial position of each loop is taken to correspond

to the turns and counter-turns that are on the side opposite to the current reversal loop. The axial position of each loop is taken to accommodate the distance between turns and counter-turns, extra half turn and counter-turn, in 3D. Geometry of the 2D inductor is presented below in the section of results, (fig. 2).
The different positions (b_1, z_1), (b_2, z_2), (b_3, z_3), (b_4, z_4), ($b_{n,1}$, $z_{n,1}$) and ($b_{n,2}$, $z_{n,2}$) are respectively, in mm, (5.5, 1.75), (6.5, 5.25), (7.5, 8.75), (8.5, 12.25), (6.2, 22.0938) and (6.2, 25.5938).

Table 2: Indication for geometry of the EM coil, in 3D

Parameters of EM coil in three dimensions, mm	
Screw thread (1)	3.5
Turns radius growth (2)	2
Counter-turns radius growth (3)	0
Turns/Counter-turns average distance (4)	7.5
Inner Turns diameter	7.5–>14.5
Inner Counter-turns diameter	10.4
Current reversal loop length (5)	22

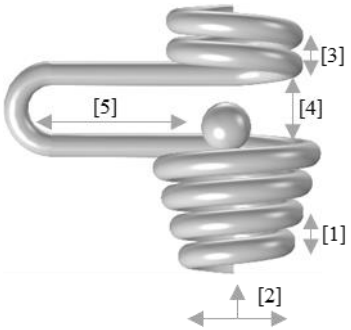

Figure 1: Geometry of a 3D inductor with parameters given in the Table 2.

Results and discussion

Calculations, performed with different software in 2D axially symmetric configuration (fig.2a) demonstrate qualitative similar distribution both for the axial component of the Lorentz force (fig.2b) and for the Joule heating (fig.2c) in the sample. Moreover, the value for the Lorentz force obtained analytically with eq.(2) and numerically with eq.(5) and an analogous calculation in COMSOL Multiphysics® are very close inside the coils apart its bottom part. The values of the Joule heating calculated with MIMEF and COMSOL Multiphysics® are very close and are always above zero, the minimal value obtained for the smallest sample is ~4.7W. Yet, the value of $Q_J(z)$ obtained with analytical approach tends to zero in the area where EM fields produced by the upper and lower parts of the coil nearly compensate each other. This is not surprising since analytical solution given by eq.(2) corresponds to the Joule heating of a sphere placed in a uniform magnetic field whereas the latter strongly varies in the gap between the upper and the bottom part of the coil.

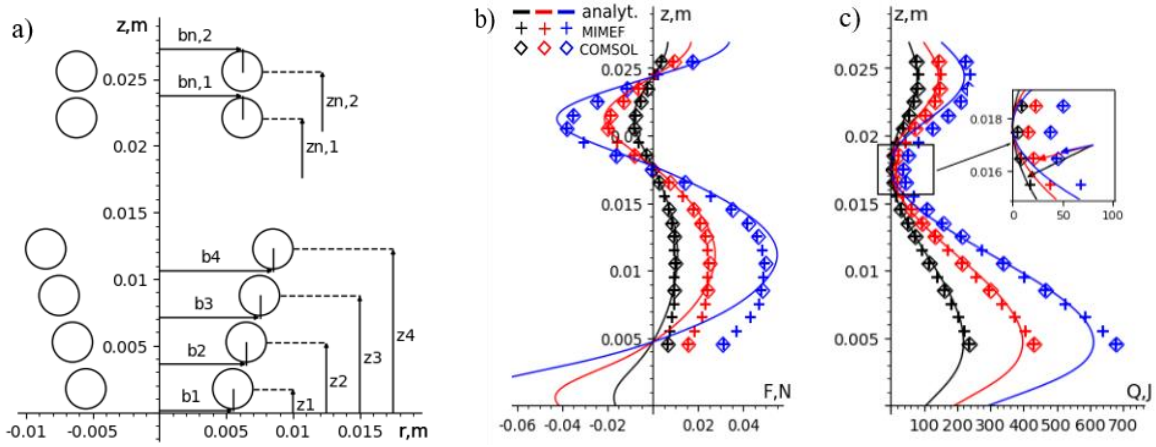

Figure 2: Geometry of the 2D axially symmetric inductor a), parameters are given after Table 1; Results obtained for 2D axially symmetric calculations: b) axial component of the total Lorentz force acting on the sample placed at various axial position; c) total Joule power released in the sample placed at various axial position. In (b) and (c) black, red and blue colors are for a=2.5mm, a=3mm and a=3.5mm, respectively.

All calculation methods indicate equilibrium position of the sample a little below the center of the gap between the upper and bottom part of the coil ($z_c \approx 17.2$mm), the larger is the sample, the higher is its position (Table 3). This happens because deformation of the sample is not taken into account, consequently, larger sample happens to be closer to the coil and is subjected to the stronger Lorentz force which pushes it higher. A difference in results obtained in MIMEF calculations with two different approaches is a numeric artefact and seems to be minor with respect to the sample size. Yet, surprisingly, it leads to quite different Joule heating that results in temperature difference $T_{\sum F=0} = 1831$K vs $T_{\min(W)} = 1722K$ for a=2.5mm and $T_{\sum F=0} = 1981$ K vs $T_{\min(W)} = 2022K$ for a=3.5mm.

Table 3: Results of calculations in two-dimension

	Equilibrium position, mm			**Joule heating, W**		
	a=2.5mm	a=3mm	a=3.5mm	a=2.5mm	a=3mm	a=3.5mm
Analytical approach	15.7	16.4	16.7	12.168	9.757	9.296
MIMEF, [$\sum$ F = 0]	15.6	16.3	16.5	16.434	22.879	44.223
MIMEF, [min(W_g+W_m)]	15.9	16.2	16.3	12.916	24.246	48.010
COMSOL, [$\sum$ F = 0]	15.6	16.3	16.5	16.516	22.989	44.412

Results presented below are for a sample with the size a=3mm and are based on numerical modeling performed in 3D with COMSOL Multiphysics®. The 3D numerical calculations are only done with COMSOL in order to use a more complete model. It is found that the axial position of the sample remain close to that found with 2D calculation: 16.25 mm vs 16.27 mm, but the sample is slightly displaced with respect to the vertical axis of the helicoid (fig. 3a). Displacement in the plane (x, z) is minor (0.32 mm) while in the plane (y, z) it happens to be toward the reversal loop (1 mm). Consequently, the fluid flow loses its symmetry in the (y, z) plane (fig. 3b) while in the plane (x, z) two vortices, known from axisymmetric simulations, persist [11].

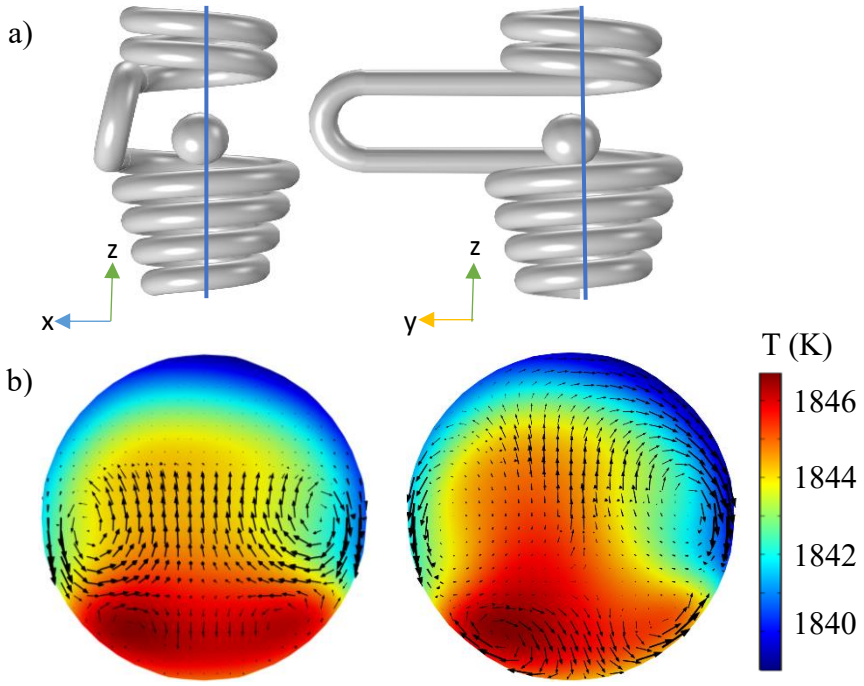

Figure 3: Results obtained for 3D calculations (COMSOL) for Ni (a=3mm): a) Equilibrium position; b) velocity and temperature field distribution.

The average temperature of the sample is slightly different between 2D (1828 K) and 3D (1846 K) calculations.

Experimental and numerical comparisons

The coil used in the experimental setup corresponds exactly to the one used in numerical modelling due to the utilization of a template fabricated via the 3D printing. The generator adapts the frequency of the AC current according to the properties of the load, the latter is composed of the inductor and the sample: for all load's sizes, $f = 151$ kHz. The effective current measured with a Rogowski sensor is $Ieff = 340 \pm 10$ A, depending of measurement and load size. For numerical calculations in 3D the effective current is adapted to correspond to the values found experimentally. The temperature is acquired with a bichromatic pyrometer at which emissivity of the sample is adjusted for $\varepsilon = 0.33$. The measurement of the equilibrium positions involved the use of an ultra-fast camera (506 fps at 1280x1024 px) to obtain a sequence of images (fig. 4a). Image processing with Fiji [12] starts with filtering, which is necessary for edges clarity. A shape analysis made with the *hull and circle* [13] (fig. 4b) plugin, after thresholding, allows to recreate the sphere (cause of the part hidden by the coils) and thus identify the location of gravity center of the droplet which is then averaged over the image sequence.

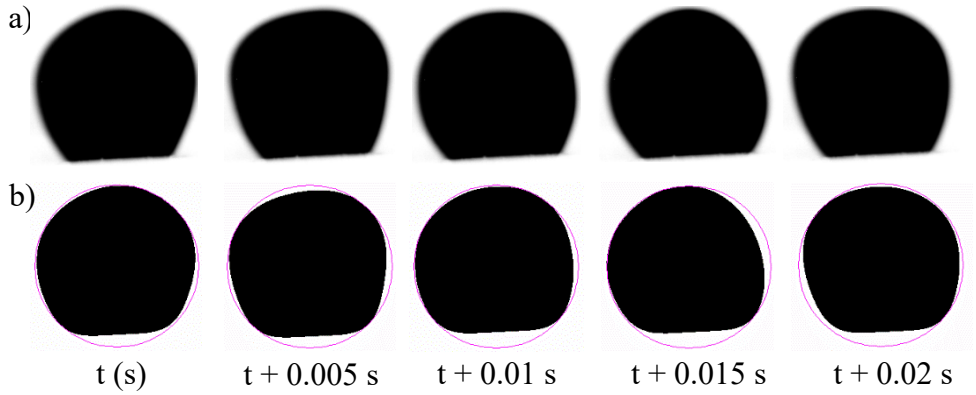

Figure 4: Image sequence of an experimental load in levitation and image analysis, in (*y*, *z*) plane: a) image captured directly with the camera; b) after filtering and hull and circle.

The use of *hull and circle* (fig. 4b), is not the best approach because the load actually is not spherical due to vibratory and oscillatory effects, as can be seen in the last two images (fig. 4b). Also, the deformation of the larger droplet because of the gravity becomes important. This implies that the coordinates found for the mean gravity center may be skewed that can lead to certain discrepancy when comparison of the numerical and experimental results is made. To estimate this discrepancy, the equilibrium position of the sample determined from the experiment is also used in numerical simulation, in particular, to find numerically the temperature of the sample. These results, obtained numerically for the sample location determined experimentally are referred below as "Exp Num" while for numerical and experimental results the references "Num" and "Exp", are used respectively.

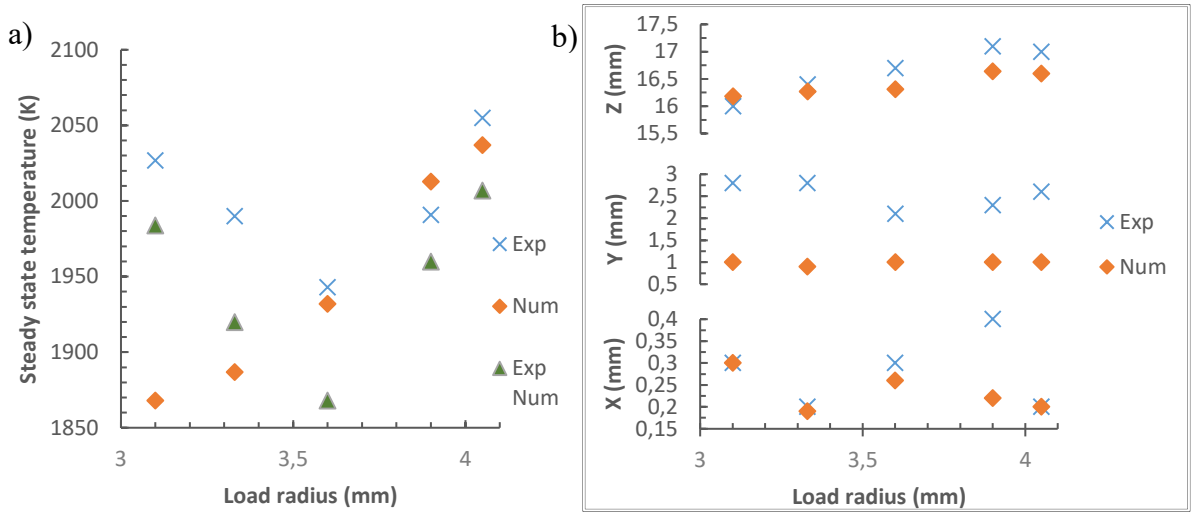

Figure 5: Experimental (Exp) and numerical (Num) results obtained for Ni (a=3.1 – 4.05 mm): a) Steady state temperature (K) for experimental (Exp) and numerical (Num) equilibrium positions and numerically with data found experimentally (Exp Num); b) Equilibrium positions found with image analysis for the experience (± 0.4 mm) and COMSOL in 3D.

The experimentally and numerically (Exp end ExpNum) defined temperatures (fig. 5a) follow the similar variation for loads of different sizes, with the highest temperatures for the smallest and the largest samples. This non-monotone temperature variation is a result of combinations of several factors that are: the distance between the sample and the coil, the total surface of the sample and its volume heated with the eddy current. The difference in temperature between experimental and numerically (Exp end ExpNum) can be explained because the sample deformation is not taken into account in the numerical calculations. Regarding the equilibrium positions (fig. 5b), the experimental and numerical positions along the *z*-axis follow the same trend and are close. For *x*-axis, the values are almost identical except for the fourth size. Regarding the *y*-axis, numerical results do not show that the sample displacement decreases from the first to the third size of the load and increases thereafter. Furthermore, the values obtained experimentally, for *y*, are larger.

Conclusions

Analytical approach well predicts the distribution of the vertical component of the Lorentz force along the axis of the coil but failed in the estimation of the Joule power and, further, the temperature of the sample. Consequently, optimization for the axial position of the sample for various geometry of the inductor can be done at the first stage using analytical solution. The problem is, however, that the latter does not take into account the radius of the coil tube, some precautions are required to avoid unrealizable configurations. Surprising results of simulations performed with MIMEF and COMSOL Multiphysics® is that the temperature of the sample strongly depends on the position of the sample inside the coil but is similar for 2D and 3D simulations. Because of a rather large skin depth, and simple configuration, the advantages of using MIMEF versus COMSOL Multiphysics® are not decisive. Overall, since 3D calculations are more time consuming, it is reasonable to use them at the second stage of the inductor optimization, in order to approach axial symmetry for the electromagnetic field and avoid sample hiding by inductor's turns, because it is important for more accurate analysis of experimental data. If deformation of the sample is not taken into account in the numerical simulations, then the equilibrium position of the sample found numerically differs from

experimental one that also leads to different temperature definition. This can be overcame if the equilibrium position of the sample determined from the experiment is used in numerical simulations, then the trend in temperature variation with the size of the sample observed numerically and experimentally is similar.

Acknowledgements

This work acknowledge the support from CNES for access to the data obtained in microgravity and used in simulations.

REFERENCES

[1] I. EGRY, G. LOHOEFER, G. JACOBS. Surface tension of liquid metals: Results from measurements on ground and in space. *Phys. Rev. Lett.*, 75 (1995), no. 22, pp. 4043–4046.
[2] D. M. MATSON, X. XIAO, J. E. RODRIGUEZ, J. LEE, and al. Use of thermophysical properties to select and control convection during rapid solidification of steel alloys using electromagnetic levitation on the space station. *JOM*, 69 (2017), pp. 1311–1318.
[3] M. ADACHI, Y. YAMAGATA, M. WATANABE, S. HAMAYA, M. OHTSUKA, H. FUKUYAMA. Composition dependence of normal spectral emissivity of liquid Ni–Al alloys. *ISIJ Int.*, 61 (2021), no. 3, pp. 684–689.
[4] M. MOHR, R. K. WUNDERLICH, K. ZWEIACKER, S. PRADES-RÖDEL, and al. Surface tension and viscosity of liquid Pd43Cu27Ni10P20 measured in a levitation device under microgravity. *NPJ Microgravity*, 5 (2019) no. 1, pp.1–8.
[5] M. MOHR, D. C. HOFMANN, H.-J. FECHT. Thermophysical properties of an Fe57.75Ni19.25Mo10C5B8 glass-forming alloy measured in microgravity. *Adv. Eng. Mat.*, 23 (2021), no. 3, pp. 2001143.
[6] E. FROMM and H. JEHN. Electromagnetic forces and power absorption in levitation melting. *Brit. J. of Appl. Phys.*,16 (1965), no. 5, pp. 653–663.
[7] W. R. SMYTHE. Static and dynamic electricity. (McGrAW-HILL BOOK COMPANY, Inc.,1950)
[8] A. GAGNOUD, Y. DU TERRAIL-COUVAT, and O. BUDENKOVA. 3D numerical modeling for inductive processes, *Conf. Series: Mat. Sci. Eng.*, 424 (2018), pp. 012045.
[9] COMSOL Multiphysics® v. 5.6. www.comsol.com. COMSOL AB, Stockholm, Sweden.
[10] A. DIARRA. Measurements of thermal properties of metals using electromagnetic process. PhD thesis, 2016, University Grenoble Alpes.
[11] O. BUDENKOVA, Y. DELANNOY, A. GAGNOUD. Numerical simulations of turbulent flow in an electromagnetically levitated metallic droplet using k-Ω SST and Reynolds stress models. *Magnetohydrodynamics*, 56 (2020), no. 2-3, pp. 203-214.
[12] J. SCHNINDELIN *and al.* Fiji: an open-source platform for biological-image analysis. *Nat. Methods*, vol. 9, no.7, pp. 676-682.
[13] A. KARPERIEN, S. C., and R. ROY., *Hull and Circle.*